ADVANCED MATERIALS

# Ductile Bulk Metallic Glass Foams**

By *Alan H. Brothers* and *David C. Dunand**

Metallic foams exhibit high density-compensated strength and energy-absorption capacity,[1–3] making them useful as ultralight structural materials[1–3] and bone-replacement implants.[4] Bulk metallic glasses (BMG) combine exceptional strength, elasticity, wear, and corrosion resistance with modest densities and low processing temperatures,[5] and are being considered for structural applications and biocompatible implants.[6] Thus, a BMG foam may offer unique opportunities in engineering structures or biomedical implants.

Although Apfel and Qiu[7] suggested a potential BMG-foaming process as early as 1996, it was not until 2003 that Schroers et al.[8] successfully foamed the BMG $Pd_{43}Ni_{10}Cu_{27}P_{20}$ using water vapor released during decomposition of a hydrated $B_2O_3$ flux. The same alloy was later foamed by Wada and Inoue[9] by casting around granular NaCl, followed by dissolution of the NaCl. Shortly thereafter, Brothers and Dunand[10] reported the first method for foaming commercial Zr-based BMG alloys using melt infiltration of hollow carbon microspheres.

Given that monolithic BMG rarely exceeds 2 % compressive strain to failure,[5] it is unclear whether BMG foams can achieve the high levels of compressive ductility expected of crystalline metal foams. The first evidence supporting such a possibility was provided by Conner et al.,[11] who compiled literature documenting high bending ductility (10–100 %) in amorphous metal foils and wires with submillimeter thickness, which was attributed to decreases in both shear band spacing and shear offset per band as sample dimension was reduced. The similarity between wires deformed in bending and the bending of thin struts within a foam deformed in compression motivates the hypothesis that amorphous metal foams should be ductile in compression. Although the Pd-based BMG foam described by Wada and Inoue[9] was reportedly compressed to 90 % nominal strain without failure, its behavior more closely resembled that of brittle foams than conventional metal foams;[1] in this report, we describe mechanical behavior of a Zr-based BMG foam closely resembling that of comparable Al-based foams, demonstrating that BMG foams can be made to behave like their ductile crystalline counterparts.

The processing technique developed here is a variant of the replication method used previously in the production of crystalline metal foams[12–15] (as well as the Pd-based BMG foam of Wada and Inoue[9]), in which the alloy is cast into a bed of leachable salt that is subsequently dissolved after solidification. The placeholder in this work was $BaF_2$, chosen for its high stability and melting point, and the alloy was Vit106 ($Zr_{57}Nb_5Cu_{15.4}Ni_{12.6}Al_{10}$), which ranks among the best metallic glass formers containing neither precious metals nor toxic beryllium. Casting of molten Vit106 into a sintered $BaF_2$ pattern was performed using low-pressure melt infiltration followed by rapid quenching, and leaching was accomplished by immersion of the Vit106/$BaF_2$ composite in a bath of 2 M nitric acid.

Scanning electron microscopy (SEM) images of an open-cell Vit106 foam of diameter $4.47 \pm 0.002$ mm and height $8.66 \pm 0.005$ mm, following pattern removal and thinning to a density of 1.52 g cm$^{-3}$ (78 % porosity), are shown in Figure 1. The foam structure is macroscopically homogeneous (Fig. 1a) with a uniform pore size corresponding to the mean salt-particle size of 212–250 μm, and is very similar to that of aluminum foams produced using sintered NaCl patterns, with angular pores and a large fraction of the alloy localized at the nodes between struts.[14] All Vit106 struts (Fig. 1b) are well below the critical thickness (~1 mm) for which high bending ductility is expected.[11] Figure 1c shows the macrostructure of the foam following uniaxial compression to 50 % strain, and Figures 1d–f display representative struts from the deformed foam. Some struts (Fig. 1d) exhibit evidence of shear lips formed by shear band motion with little or no cracking, while others (Fig. 1e) contain both shear bands and incipient cracks, and a few (Fig. 1f) display fracture with no evidence of shear banding.

A slice of the sample shown in Figure 1 was tested for crystallinity using X-ray diffraction (XRD). As shown in Figure 2, no crystalline phases were present in the foam (within the limits of XRD detection), which is important not only to the mechanical properties of the foam, but also to its resistance to localized corrosion during leaching in the acid bath.

The uniaxial compressive behavior of the foam represented in Figures 1,2 was linear to a strain of ca. 2 %, with yielding at ca. 21 MPa (Fig. 3). Yielding in ductile metallic foams is associated with plastic collapse of the struts within the foam. For elastic-perfectly plastic materials with no significant tension–compression asymmetry (e.g., Al), the plastic-collapse moment is directly proportional to yield strength; for elastic-perfectly plastic materials with significant asymmetry (e.g., Vit106, whose tensile- and compressive-yield strengths are 1200 MPa and 1800 MPa, respectively[16]), the corresponding value from beam theory[17] is the harmonic mean of tensile and compressive strengths, 1440 MPa in the case of Vit106. Using this value in the semi-empirical model of Gibson and Ashby[1] shows that the measured yield stress is lower, by a factor of about two, than the predicted value of 46 MPa. This discrepancy can be explained by the fact that the model assumes that nodes are no thicker than struts, and thus predicts a higher load-bearing efficiency than the current foam (which has thickened nodes) for a given relative density.

[*] Prof. D. C. Dunand, A. H. Brothers
Department of Materials Science and Engineering
Northwestern University
Evanston, IL 60208 (USA)
E-mail: dunand@northwestern.edu

[**] This work was supported by the Defense Advanced Research Project Agency's Structural Amorphous Metals (DARPA-SAM) program and the Caltech Center for Structural Amorphous Metals. The authors thank Richard Scheunemann (Northwestern University) for experimental help in preform fabrication and John DeFouw (Northwestern University) for useful discussions.

  DOI: 10.1002/adma.200400897 

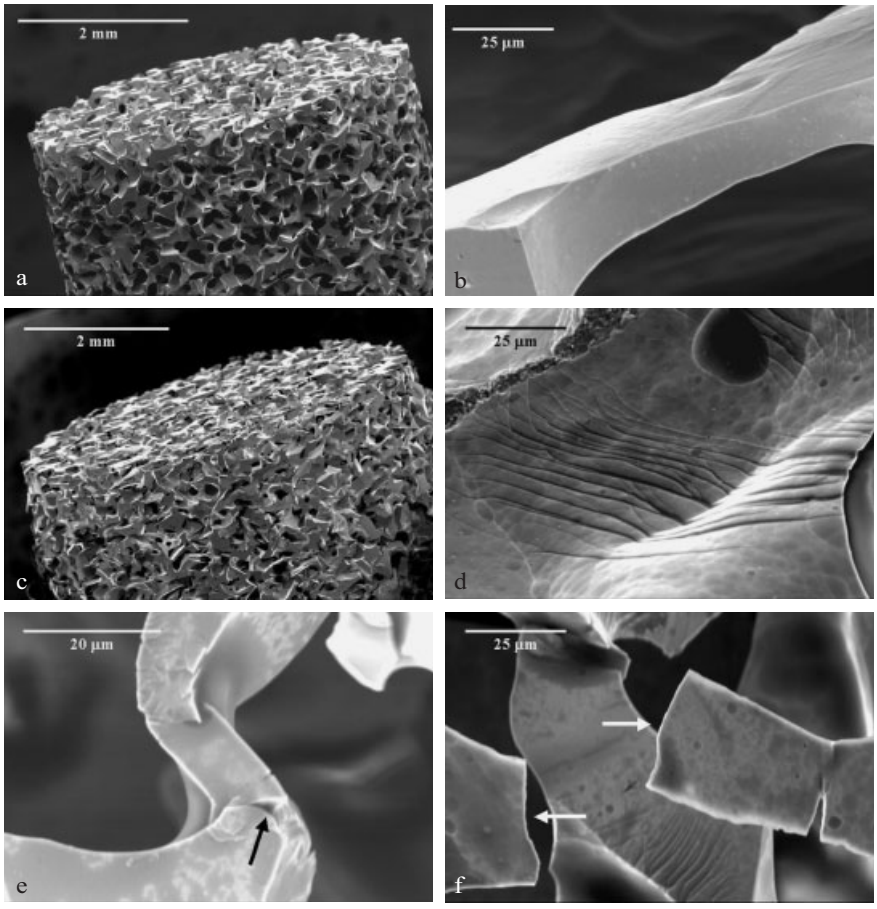


**Figure 1.** SEM images of an amorphous Vit106 foam with 22 % relative density. a) Macrostructure of the foam prior to compression. b) Individual strut within the undeformed foam. c) Macrostructure of the foam after 50 % compression. d) Deformed strut in the compressed foam, showing evidence of ductility in the form of shear lips, caused by intersection of shear bands with free surfaces. e) Buckled strut in the compressed foam, showing evidence of shear bands as well as incipient cracks (indicated by an arrow). f) Fractured strut in the compressed foam, exhibiting fracture with no shear bands. Mating fractured surfaces are indicated by arrows.

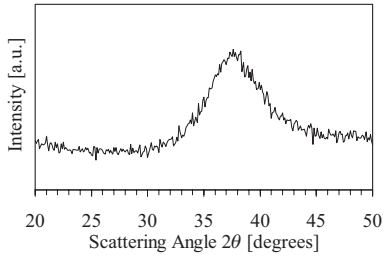


**Figure 2.** XRD pattern taken from a slice of the Vit106 foam depicted in Figure 1a. The pattern shows a characteristic amorphous feature with no evidence of either $BaF_2$ or native crystalline phases.

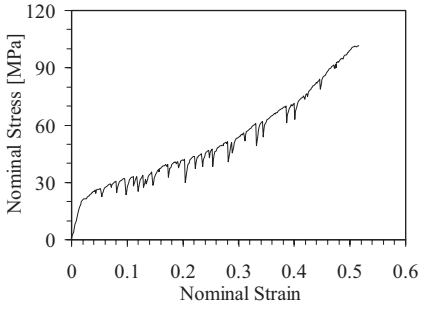


**Figure 3.** Compressive stress–strain behavior of the 22 %-dense Vit106 foam shown in Figure 1a. The foam was unloaded from 50 % engineering strain without macroscopic failure (Fig. 1c).

After yielding, the flow stress increased gradually to 100 MPa at a strain ca. 50 %, with the sample remaining intact after unloading. Monotonically increasing flow stress after yield is a feature of higher relative-density metallic foams,[3] and was previously observed in a pure aluminum foam of the same relative density (22 %) and similar architecture (produced by infiltration of sintered NaCl).[14] At high strains (> 10 %), this stress increase results from contact among deformed struts and nodes, and is therefore most pronounced in foams having high mass localization at cell nodes, such as those produced by salt replication. At lower strains (< 10 %), the increase of flow stress in aluminum foam was attributed to

  

ADVANCED MATERIALS

work-hardening;[14] it is unlikely that this explanation applies to the Vit106 foam, however, as BMG exhibits little or no work-hardening. More likely, contact among nodes and struts accounts for increasing flow stress over the entire range of strains considered here, as the spacing between the thick nodes of the Vit106 foam is smaller than would be predicted based on density, due to the preferential removal of material from high-surface-area struts during pattern removal.

While the flow stress of aluminum foams increases smoothly with plastic strain after yielding,[14] that of the Vit106 foam is punctuated by sharp stress drops followed by recovery (Fig. 3). Since no evidence of brittle crystalline inclusions was found (Fig. 2), and since all the foam features are well below the critical embrittling thickness of ~1 mm,[11] these serrations are believed to arise from tensile strut fracture, illustrated in Figure 1f. While the ductility of aluminum struts does not depend crucially on deformation mode, that of Vit106 struts is limited to bending deformation. Aluminum struts with aspect ratios and/or orientations favoring axial deformation remain ductile, while Vit106 struts under similar conditions fail by shear banding at high stress and low strain. We believe that the serrations of Figure 3 reflect such brittle failures, and the subsequent redistribution of stress among neighboring ductile struts loaded in bending; this view is supported by the decreased frequency of serrations at high strains where most of the brittle, axially-loaded struts are expected to have failed.

BMG foams such as those presented here show potential both as ductile, lower-density alternatives to monolithic glassy alloys and stronger, more processable alternatives to foams made from high-strength crystalline alloys. However, their success as structural materials or biomedical implants depends crucially on the achievement of ductility. In this communication, we described synthesis of open-cell BMG foams and demonstrated that amorphous metallic foams can achieve high compressive ductility (comparable to ductile crystalline metal foams) through strut bending, in sharp contrast to the brittle compressive and bending behavior of BMG in bulk form.

## *Experimental*

Optical-grade (99.999 %+) $BaF_2$ was crushed in a mortar and pestle, sieved to isolate 212–250 μm particles, packed into graphite crucibles (packing density 50 ± 2 %), and sintered into patterns for 10 h at 1250 °C under high vacuum. Patterns of 7 mm diameter were placed within thin-walled (0.75 mm) stainless steel crucibles and vacuum dried at 300 °C for at least 30 min in a tube furnace. Crucibles evacuated to $2 \times 10^{-5}$ torr (1 torr ≈ 133 Pa) were preheated for 3 min at 975 °C. Pre-alloyed Vit106 charges were then lowered onto the patterns under high vacuum and melted for 3 min to promote a gas-tight seal between the melt and crucible wall. After melting, a pressure of 50 kPa of high-purity argon gas was applied to drive the melt into the open spaces of the salt pattern. This pressure was maintained for 60 seconds to promote complete infiltration, after which the crucibles were immersed in a large bath of strongly agitated, chilled brine solution (8.5 wt.-% NaCl in water). To ensure radial cooling throughout the samples, the bottoms of the steel crucibles were made seven times thicker than their walls. Following infiltration, a $BaF_2$/Vit106 composite was ground on a diamond abrasive wheel to a final diameter of 4.5 mm. The faces of the sample were cut flat and parallel using a diamond saw, such that the sample aspect ratio was 1.9. The salt pattern was leached out by immersion of the composite in an ultrasonically agitated bath of 2 M nitric acid for a period of ~4 h, interrupted periodically to refresh the bath. Immersion in the bath was extended for an additional 12 h following salt removal until the sample reached a target relative density of 20–25 %. XRD analysis of the sample was performed using Cu Kα radiation (Scintag XDS 2000). SEM images were taken with a Hitachi S-3500N scanning electron microscope using secondary electron imaging. Compressive testing was performed under displacement control at a nominal strain rate of $5 \times 10^{-4}$ $s^{-1}$ on a Sintech 20/G screw-driven mechanical testing apparatus outfitted with a compressive cage that ensured sample parallelism.

Received: June 4, 2004
Final version: October 12, 2004

[1] L. J. Gibson, M. F. Ashby, *Cellular Solids: Structure and Properties*, 2nd ed., Cambridge University Press, Cambridge, UK **1997**.
[2] J. Banhart, *Prog. Mater. Sci.* **2001**, *46*, 559.
[3] M. F. Ashby, A. G. Evans, N. A. Fleck, L. J. Gibson, J. W. Hutchinson, H. N. G. Wadley, *Metal Foams: A Design Guide*, Butterworth-Heinemann, Boston, MA, USA **2000**.
[4] S. N. Parikh, *Orthopedics* **2002**, *25*, 1301.
[5] W. H. Wang, C. Dong, C. H. Shek, *Mater. Sci. Eng.* **2004**, *44*, 45.
[6] S. Hiromoto, K. Asami, A. P. Tsai, T. Hanawa, *Mater. Trans.* **2002**, *43*, 261.
[7] R. E. Apfel, N. Qiu, *J. Mater. Res.* **1996**, *11*, 2916.
[8] J. Schroers, C. Veazey, W. L. Johnson, *Appl. Phys. Lett.* **2003**, *82*, 370.
[9] T. Wada, A. Inoue, *Mater. Trans.* **2003**, *44*, 2228.
[10] A. H. Brothers, D. C. Dunand, *Appl. Phys. Lett.* **2004**, *84*, 1108.
[11] R. D. Conner, W. L. Johnson, N. E. Paton, W. D. Nix, *J. Appl. Phys.* **2003**, *94*, 904.
[12] L. Polonsky, S. Lipson, H. Markus, *Mod. Cast. (1956–66)* **1961**, *39*, 57.
[13] C. San Marchi, A. Mortensen, in *Handbook of Cellular Metals: Production, Processing, Applications* (Eds: H.-P. Degischer, B. Kriszt), Wiley-VCH, Weinheim, Germany **2002**.
[14] C. San Marchi, A. Mortensen, *Acta Mater.* **2001**, *49*, 3959.
[15] Y. Y. Zhao, D. X. Sun, *Scr. Mater.* **2001**, *44*, 105.
[16] H. Choi-Yim, R. D. Conner, F. Szuecs, W. L. Johnson, *Acta Mater.* **2002**, *50*, 2737.
[17] M. Jirásek, Z. P. Bazant, *Inelastic Analysis of Structures*, Wiley, New York **2002**.

  